Available Online

JSR Publications

J. Sci. Res. **14** (2), 641-658 (2022)

JOURNAL OF SCIENTIFIC RESEARCH

www.banglajol.info/index.php/JSR

Synthesis and *in vitro* Biological Studies of Copper Complexes Derived from Some Novel Hetero-Organoselanylquinoline Ligands

P. Moohambihai*, K. Nagashri

Department of Chemistry, Manonmaniam Sundaranar University, Tirunelveli-627012, Tamilnadu, India

Received 11 December 2021, accepted in final revised form 15 March 2022

Abstract

A set of copper(II) complexes (3a-i) comprises (16*E*)-N-(2-phenylquinolin-4(1*H*)-ylidene)-3-(phenlselanyl)pyridine-2-amine (L^1-L^3), (16*E*)-2,6-dimethyl-N-(2-phenylquinolin-4(1*H*)-ylidene)-5-(phenlselanyl)pyrimidine-4-amine (L^4-L^6), 16*E*)-N-(2-phenylquinolin-4(1*H*)-ylidene)-2-(phenylselanyl)*H*-imidazo[1,2-α]pyridine-3-amine (L^7-L^9) ligands were synthesised and characterised using spectroscopic techniques. The metal-to-ligand 1:1 stoichiometry of prepared copper complexes was confirmed by mass spectra. The Cu(II) ion produces complexes with a distorted square planar, according to UV–Vis and ESR spectroscopy studies. The antioxidant activity of these complexes has been determined. The cytotoxic potential of the complexes was also investigated in vitro. The complex 3f was found to have significant cytotoxicity against MCF-7. The DNA binding characteristics of copper(II) complexes were investigated. The findings indicate that the complexes interacted with the calf thymus (CT-DNA). In addition, the complexes were tested *in vitro* for antimicrobial activity against three Gram-negative bacteria, three Gram-positive bacteria, and three Fungi.

Keywords: Antimicrobial; Antioxidant; Cytotoxicity; DNA binding; Hetero-organoselanylquinoline.

doi: http://dx.doi.org/10.3329/jsr.v14i2.56544 J. Sci. Res. **14** (2), 641-658 (2022)

1. Introduction

Because of their straightforward synthesis, versatility, and diverse range of uses, coordination complexes have remained a significant and popular area of research. Transition metal complexes appear to have played a key role in the evolution of coordination chemistry [1]. It also plays a significant role in biological processes, as evidenced by the fact that metal ions are known to activate enzymes. Many metal complexes are used in microelectronics and pharmaceuticals [2]. Metal complexes have a wide range of applications in various domains of human curiosity, depending on the

*Corresponding author: ambikachem12@gmail.com

nature of the metal and the type of ligand [3]. Quinolines are nitrogen heterocycles found in many natural and synthetic compounds. They have antibacterial [4], antifungal [5], antileishmanial [6], antimalarial [7], antitumor [8], anticonvulsant, and antihypertensive [9] properties.

Since the 1970s, synthetic organoselenium compounds have piqued synthetic chemistry's interest. Some reports describe the discovery of various selenoproteins involved in various physiological processes in mammals, including thyroid hormone production, antioxidant defense, and immune responses. Synthetic organoselenium compounds have also been reported to behave as antioxidants, chemo preventers, and apoptotic inducers in the brain, liver, skin, colon, lung, and prostate [10,11]. In the research field, selenium becomes active when it reacts with heterocycles such as pyridine, pyrimidine, and imidazopyridine. The use of a selenium atom as a building block for a range of five- and six-membered selenium-containing heterocyclic compounds necessitates additional consideration. Selenium has been associated with antioxidant, anti-inflammatory, and cytostatic activities [12,13]. Antioxidant activity is connected to the amount of selenium in several antioxidant enzymes that protect cells from oxidative damage [14]. Organo-selenium compounds have been employed as organic conductors, semiconductors, and optoelectronics in addition to their prospective applications [15,16]. We decided to investigate the synthesis and biological properties of Schiff base copper complexes derived from organoselenium (2-(phenylselanyl)pyridine-3-amine, 2,6-dimethyl-5-(phenylselanyl)pyrimidin-4-amine, 2-(phenylselanyl)*H*-imidazo[1,2-α] pyridine-3-amine ligands to design better drugs that target cellular DNA. In addition, the antibacterial activity, DNA binding investigations, antioxidant and cytotoxicity properties of the generated complexes were investigated

2. Experimental

In this experiment, AnalaR grade chemicals were employed. The NMR spectra were recorded using tetramethylsilane (TMS) as an internal standard. In comparison to TMS, chemical changes are measured in parts per million. The ligands and their complexes' Fast Atom Bombardment (FAB) mass spectra were recorded on a Jeol SX 102/DA-6000 mass spectrometer/data system using argon/xenon (6 kV, 10 mA) as the FAB gas. The molar conductance of copper complexes in dimethylsulphoxide (DMSO) solution was measured using a coronation digital conductivitymeter. The IR spectra of the ligands and their copper complexes were measured in the 4000–200 cm^{-1} range using a KBr disc on a Perkin–Elmer 783 spectrophotometer. The magnetic susceptibility values were calculated using the equation eff = 2.83 (m.T) 1/2. The diamagnetic adjustments were made using Pascal's constant, and the calibrant was Hg[Co(SCN)4]. On a Varian E112 X-band spectrometer, the copper complexes' ESR spectra were obtained at 300 and 77 K.

2.1. *Preparation of ligands 2a-i (L^1-L^9)*

2-(phenylselanyl)pyridine-3-amine, 2,6-dimethyl-5-(phenylselanyl)pyrimidin-4-amine, 2-(phenylselanyl)H-imidazo[1,2-α]pyridine-3-amine were separately mixed with 12 mmolof sodium borohydride in 50 mL of DMF with continuous stirring at 0-5 °C. After dilution with an equal volume of DMF, 10 mmol of phenylquinoline compounds 1(a-i) were added dropwise to the resultant solution. The reactions were done in 60-90 min. The extractions were carried out in dichloromethane under a vacuum. Before being dried over anhydrous sodium sulfate, the organic layer was washed multiple times with brine solution. The solvent was extracted using a rota evaporator, and the liquid was purified using a silica column and chloroform-methanol (8:2) as the eluant.

2.1.1. *2a (16E)-N-(2-phenylquinoline-4(1H)-ylidene)-3-(phenylselanyl)pyridine-2-amine*

Yield: 68 %. Anal.calcd for $C_{26}H_{19}N_3Se$: C, 69.03; H, 4.33; N, 9.29; Found: C, 69.01; H, 4.31; N, 9.27. FAB mass spectrometry (FAB-MS) *m/z* 454[M+1].^{1}H NMR (400 MHz, $CDCl_3$, *δ*, ppm): 6.15 (s, 1H), 6.52-6.73 (m, 5H), 6.82-6.91 (m, 3H), 7.26-7.28 (d, 2H), 7.60-7.64 (m, 3H), 8.23-8.72 (m, 4H), 8.82 (s, -NH). ^{13}C-NMR (400 MHz, DMSO-d_6): 138.1 (C-2), 102.3 (C-3), 164.4 (C-4), 130.2 (C-5), 118.7 (C-6), 131.6 (C-7), 116.1 (C-8), 148.2 (C-9), 117.6 (C -10), 134.2 (C-11), 126.2 (C-12, C-16), 128.5 (C-13, C-15), 127.8 (C-14). 174. 8 (C-18), 150.4 (C-20), 122.3 (C-21), 137.1 (C-22), 117.1 (C-23), 129.8 (C-25), 131.4 (C-26, C-30), 128.6 (C-27, C-28, C-29).

2.1.2. *2b (4E)-4-(3-(phenylselanyl)pyridine-2-ylimine)-1,4-dihydro-2-phenylquinoline-7-ol*

Yield: 68 %. Anal.calcd for $C_{26}H_{19}N_3OSe$: C, 66.67; H, 4.09; N, 8.97; Found: C, 66.64; H, 4.05; N, 8.94. FAB mass spectrometry (FAB-MS) *m/z* 470 [M+1].^{1}H NMR (400 MHz, $CDCl_3$, *δ*, ppm): 4.84 (s, -OH), 5.88 (s, 1H), 5.92 (d, 1H), 6.12 (s, 1H), 6.34 (d, 1H) 6.50-6.63 (m, 5H), 6.78-6.84 (m, 3H), 7.24-7.26 (d, 2H), 7.58-7.62 (m, 3H), 8.64 (s, -NH). ^{13}C-NMR (400 MHz, DMSO-d_6): 138.1 (C-2), 102.1 (C-3), 164.4 (C-4), 131.2 (C-5), 106.4 (C-6), 161.4 (C-7), 101.1 (C-8), 149.2 (C-9), 110.4 (C-10), 134.2 (C-11), 126.2 (C-12, C-16), 128.5 (C-13, C-15), 127.8 (C-14). 174. 8 (C-18), 150.4 (C-20), 122.2 (C-21), 136.8 (C-22), 117.1 (C-23), 129.8 (C-25), 131.4 (C-26, C-30), 128.6 (C-27, C-28, C-29).

2.1.3. *2c (16E)-N-(7-nitro-2-phenylquinoline-4(1H)-ylidene)-3-(penylselanyl)pyridine-2-amine*

Yield: 68 %. Anal.calcd for $C_{26}H_{18}N_4O_2Se$: C, 62.68; H, 3.65; N, 11.26; Found: C, 62.64; H, 3.62; N,11.24. FAB mass spectrometry (FAB-MS) *m/z* 499 [M+1]. ^{1}H NMR (400 MHz, $CDCl_3$, *δ*, ppm): 6.12 (s, 1H), 6.14 (s, 1H), 6.42 (d, 1H), 6.34 (d, 1H) 6.52-6.66 (m, 5H), 6.78-6.86 (m, 3H), 7.26-7.28 (d, 2H), 7.59-7.62 (m, 3H), 8.72 (s, -NH). ^{13}C-NMR (400 MHz, DMSO-d_6): 138.1 (C-2), 102.1 (C-3), 164.4 (C-4), 130.6 (C-5), 111.1 (C-6),

151.3 (C-7), 110.1 (C-8), 148.8 (C-9), 123.7 (C-10), 134.2 (C-11), 126.2 (C-12, C-16), 128.5 (C-13, C-15), 127.8 (C-14). 174. 8 (C-18), 150.4 (C-20), 122.2 (C-21), 136.8 (C-22), 116.8 (C-23), 129.8 (C-25), 131.4 (C-26, C-30), 128.6 (C-27, C-28, C-29).

2.1.4. *2d (16E)-2,6-dimethyl-N-(2-phenylquinoline-4(1H)-ylidene)-5-(phenylselanyl) pyrimidine-4-amine*

Yield: 68 %. Anal.calcd for $C_{27}H_{22}N_4Se$: C, 69.03; H, 4.33; N, 9.29; Found: C, 69.01; H, 4.31; N, 9.27. FAB mass spectrometry (FAB-MS) *m*/*z* 483 [M+1].^{1}H NMR (400 MHz, $CDCl_3$, δ, ppm): 2.28 (s, 6H), 6.11 (s, 1H), 6.48-6.53 (m, 5H), 7.24-7.26 (d, 2H), 7.58-7.62 (m, 3H), 8.21-8.62 (m, 4H), 8.68 (s, -NH). ^{13}C-NMR (400 MHz, DMSO-d_6): 138.1 (C-2), 102.1 (C-3), 164.4 (C-4), 129.8 (C-5), 118.7 (C-6), 131.6 (C-7), 116.1 (C-8), 147.8 (C-9), 117.6 (C-10), 134.2 (C-11), 126.2 (C-12, C-16), 128.5 (C-13, C-15), 127.8 (C-14). 181. 8 (C-18), 167.8 (C-20), 165.8 (C-22), 110.7 (C-23), 129.8 (C-25), 131.4 (C-26, C-30), 128.6 (C-27, C-28, C-29), 25.3 (CH_3 – C), 21.2 (CH_3 – C).

2.1.5. *2e (4E)-4-(2,6-dimethyl-5-(phenylselanyl)zpyrimidin-4-ylimino)-1,4-dihydro-2-phenylquinolin-7-ol*

Yield: 68 %. Anal.calcd for $C_{27}H_{22}N_4OSe$: C, 65.19; H, 4.46; N, 11.26; Found: C, 65.16; H, 4.42; N, 11.22. FAB mass spectrometry (FAB-MS) *m*/*z* 499 [M+1].^{1}H NMR (400 MHz, $CDCl_3$, δ, ppm): 2.28 (s, 6H), 4.78 (s, -OH), 6.11 (s, 1H), 6.22 (d, 1H), 6.38 (d, 1H) 6.46-6.52 (m, 5H), 6.72(s, 1H), 7.22-7.25 (d, 2H), 7.56-7.60 (m, 3H). 8.64 (s, NH).^{13}C-NMR (400 MHz, DMSO-d_6): 138.1 (C-2), 102.1 (C-3), 164.4 (C-4), 131.2 (C-5), 105.7 (C-6), 161.4 (C-7), 101.1 (C-8), 149.2 (C-9), 110.2 (C-10), 134.2 (C-11), 126.2 (C-12, C-16), 128.5 (C-13, C-15), 127.8 (C-14). 181. 8 (C-18), 167.8 (C-20), 165.8 (C-22), 110.7 (C-23), 129.8 (C-25), 131.4 (C-26, C-30), 128.6 (C-27, C-28, C-29), 25.3 (CH_3 – C), 21.2 (CH_3 – C).

2.1.6. *2f (16E)-2,6-dimethyl-N-(7-nitro-2-phenylquinoline-4(1H)-ylidene)-5-(phenyl selanyl)pyrimidine-4-amine*

Yield: 68 %. Anal.calcd for $C_{27}H_{22}N_5O_2Se$: C, 61.60; H, 4.02; N, 13.30; Found: C, 61.56; H, 4.01; N, 13.26. FAB mass spectrometry (FAB-MS) *m*/*z* 528 [M+1]. ^{1}H NMR (400 MHz, $CDCl_3$, δ, ppm): 2.28 (s, 6H), , 6.16 (s, 1H), 6.48 (s, 1H), 6.82 (d, 1H), 6.88 (d, 1H) 6.66-6.72 (m, 5H), 7.25-7.27 (d, 2H), 7.58-7.61 (m, 3H), 8.34 (s, NH). ^{13}C-NMR (400 MHz, DMSO-d_6): 138.1 (C-2), 102.1 (C-3), 164.4 (C-4), 130.6 (C-5), 110.9 (C-6), 161.4 (C-7), 151.3 (C-8), 148.8 (C-9), 123.2 (C-10), 134.2 (C-11), 126.2 (C-12, C-16), 128.5 (C-13, C-15), 127.8 (C-14). 181. 8 (C-18), 167.8 (C-20), 165.8 (C-22), 110.7 (C-23), 129.8 (C-25), 131.4 (C-26, C-30), 128.6 (C-27, C-28, C-29), 25.3 (CH_3 – C), 21.2 (CH_3 – C).

2.1.7. *2g (16E)-N-(2-phenylquinolin-4(1H)-ylidene)-2-(phenylselanyl)H-imidazo[1,2-α]pyridine-3-amine*

Yield: 68 %. Anal.calcd for $C_{28}H_{20}N_4Se$: C, 68.65; H, 4.10; N, 11.40; Found: C, 68.61; H, 4.08; N, 11.36. FAB mass spectrometry (FAB-MS) *m/z* 493 [M+1]. ^{1}H NMR (400 MHz, $CDCl_3$, δ, ppm): 6.12 (s, 1H), 6.58-6.62 (m, 5H), 6.64-6.72 (m, 4H), 7.24-7.26 (d, 2H), 7.58-7.62 (m, 3H), 8.31-8.82 (m, 4H), 8.28 (s, NH).^{13}C-NMR (400 MHz, DMSO-d_6): 138.1 (C-2), 102.1 (C-3), 164.4 (C-4), 128.6 (C-5), 118.6 (C-6), 131.7 (C-7), 116.2 (C-8), 147.8 (C-9), 117.6 (C-10), 134.2 (C-11), 126.2 (C-12, C-16), 128.5 (C-13, C-15), 127.8 (C-14). 119. 8 (C-18), 126.1 (C-20), 119.8 (C-21), 130.1 (C-22), 115.2 (C-23), 119.8 (C-24), 144.2 (C-26), 129.8 (C-28), 131.4 (C-29, C-33), 128.6 (C-30, C-31, C-33).

2.1.8. *2h (4E)-4-(2-(phenylselanyl)H-imidazo[1,2α]pyridine-3-ylimino)-1,4-dihydro-2-phenylquinolin-7-ol*

Yield: 68 %. Anal.calcd for $C_{28}H_{20}N_4OSe$: C, 66.27; H, 3.97; N, 11.04; Found: C, 66.24; H, 3.94; N, 11.01. FAB mass spectrometry (FAB-MS) *m/z* 509 [M+1].^{1}H NMR (400 MHz, $CDCl_3$, δ, ppm): 4.74 (s, -OH), 6.08 (s, 1H), 6.18 (d, 1H), 6.32 (d, 1H), 6.34 (s, 1H), 6.42-6.46 (m, 5H), 6.62-6.73 (m, 4H), 7.20-7.23 (d, 2H), 7.44-7.48 (m, 3H), 8.34 (s, NH). ^{13}C-NMR (400 MHz, DMSO-d_6): 138.1 (C-2), 102.1 (C-3), 164.4 (C-4), 131.2 (C-5), 105.8 (C- 6), 161.4 (C-7), 101.1 (C-8), 149.3 (C-9), 110.4 (C-10), 134.2 (C-11), 126.2 (C-12, C-16), 128.5 (C-13, C-15), 127.8 (C-14). 119. 8 (C-18), 126.1 (C-19), 119.8 (C-20), 130.1 (C-21), 115.2 (C-22), 119.8 (C-24), 144.2 (C-26), 129.8 (C-28), 131.4 (C-29, C-33), 128.6 (C-30, C-31, C-33).

2.1.9. *2i (16E)-N-(7-nitro-2-phenylquinolin-4(1H)-ylidene)-2-(phenylselanyl)H-imidazo[1,2-α]pyridine-3-amine*

Yield: 68 %. Anal.calcd for $C_{28}H_{19}N_5O_2Se$: C, 62.69; H, 3.37; N, 13.06; Found: C, 62.64; H, 3.34; N, 11.03. FAB mass spectrometry (FAB-MS) *m/z* 536 [M+1]. ^{1}H NMR (400 MHz, $CDCl_3$, δ, ppm): 6.28 (s, 1H), 6.40 (d, 1H), 6.42 (d, 1H) 6.44-6.46 (m, 5H), 6.64-6.74 (m, 4H), 7.22-7.24 (d, 2H), 7.46-7.48 (m, 3H), 8.22 (s, NH). ^{13}C-NMR (400 MHz, DMSO-d_6): 137.9 (C-2), 102.1 (C-3), 164.4 (C-4), 130.7 (C-5), 111.1 (C-6), 111.4 (C-7), 110.1 (C-8), 148.8 (C-9), 123.7 (C-10), 134.2 (C-11), 126.2 (C-12, C-16), 128.5 (C-13, C-15), 127.8 (C-14). 119. 8 (C-18), 126.1 (C-19), 119.8 (C-20), 130.1 (C-21), 115.2 (C-22), 119.8 (C-24), 144.2 (C-26), 129.8 (C-28), 131.4 (C-29, C-33), 128.6 (C-30, C-31, C-33).

2.2. *Preparation of metal chelates [3a-i ($CuL^1(OAc)_2$ - $CuL^9(OAc)_2$)]*

Equimolar hot ethanolic solutions of 2-(phenylselanyl)pyridine-3-amine derivative and copper acetate (0.05 M) were placed in an RB flask at RT; the reacting mixture was stirred and allowed to precipitate. The solid product was then separated with methanol and hexane and washed repeatedly. The remaining metal complexes were prepared with the

same procedure. The metal chelates were dried in vacuum desiccators over fused calcium chloride which is illustrated in Scheme 1.

3a ($CuL^1(OAc)_2$): Yield: 68 %. Anal.calcd for $C_{30}H_{25}CuN_3O_4Se$: C 56.83, H 3.97; N 6.63; Found: C 56.79; H 3.94; N 6.59. FTIR (KBr): 3166 ν(N–H), 1160 ν (C–N), 1622 ν(C=N), 540 ν(Cu–N). FAB mass: 635 m/z [M+1]. μ_{eff}(BM) = 1.84; Δ_m (mho cm^2 mol^{-1}) = 18.

3b ($CuL^2(OAc)_2$): Yield: 69 %. Anal.calcd for $C_{30}H_{25}CuN_3O_5Se$: C 55.43; H 3.88; N, 6.46; Found: C, 55.41, H, 3.84; N 6.46. FTIR (KBr): 1622 ν(C=N), 540 ν(Cu–N). FAB mass: 776 m/z [M+1]. μ_{eff} (BM) = 1.86; Δ_m (mho cm^2 mol^{-1}) = 20.

3c ($CuL^3(OAc)_2$): Yield: 67 %. Anal.calcd for $C_{30}H_{24}CuN_4O_6Se$: C 53.06, H 3.56, N 8.25, Found: C 53.03, H 3.52, N 8.22. FTIR (KBr): 1622 ν(C=N), 540 ν(Cu–N). FAB mass: 680 m/z [M+1]. μ_{eff} (BM) = 1.76; Δ_m (mho cm^2 mol^{-1}) = 18.

3d ($CuL^4(OAc)_2$): Yield: 68 %. Anal.calcd for $C_{31}H_{28}CuN_4O_4Se$: C 56.15, H 4.26, N 8.45; Found: C 56.12, H 4.23, N 8.42. FTIR (KBr): 3305 ν(O–H), 1622 ν(C=N), 540 ν(Cu–N). FAB mass: 666 m/z [M+1]. μ_{eff} (BM) = 1.86; Δ_m (mho cm^2 mol^{-1}) = 18.

3e ($CuL^5(OAc)_2$): Yield: 68 %. Anal.calcd for $C_{31}H_{28}CuN_4O_5Se$: C 54.83, H 4.16, N 8.25, Found: C 54.81, H 4.14, N 238.. FTIR (KBr): 3305 ν(O–H), 1622 ν(C=N), 540 ν(Cu–N). FAB mass: 682 m/z [M+1]. μ_{eff} (BM) = 1.86; Δ_m (mho cm^2 mol^{-1}) = 18.

3f ($CuL^6(OAc)_2$): Yield: 66 %. Anal.calcd for $C_{31}H_{27}CuN_5O_6Se$: C 52.58, H 3.84, N 9.89, Found: C 52.56, H 3.81, N 9.85. FTIR (KBr): 3305 ν(O–H), 1622 ν(C=N), 540 ν(Cu–N). FAB mass: 709 m/z [M+1]. μ_{eff} (BM) = 1.76; Δ_m (mho cm^2 mol^{-1}) = 18.

3g ($CuL^7(OAc)_2$): Yield: 68 %. Anal.calcd for $C_{32}H_{26}CuN_4O_4Se$: C 57.10, H 3.89, N 8.32, Found: C 57.06, H 3.85, N 8.28. FTIR (KBr):1622 νC=N), 540 ν(Cu–N). FAB mass: 674 m/z [M+1]. μ_{eff} (BM) = 1.76; Δ_m (mho cm^2 mol^{-1}) = 18..

3h ($CuL^8(OAc)_2$): Yield: 67%. Anal.calcd for $C_{32}H_{26}$ CuN_4O_5Se: C 55.78, H 3.80, N 8.13; Found: C 55.75, H 3.75, N 8.11. FTIR (KBr): 1622 ν(C=N), 540 ν(Cu–N). FAB mass: 690 m/z [M+1]. μ_{eff} (BM) = 1.86; Δ_m (mho cm^2 mol^{-1}) = 16.

3i ($CuL^9(OAc)_2$): Yield: 69 %. Anal.calcd for $C_{32}H_{25}CuN_5O_6Se$: C 53.52, H 3.51, N 9.75; Found: C 53.48, H 3.47, N 9.71. FTIR (KBr): 1622 ν(C=N), 540 ν(Cu–N). FAB mass: 719 m/z [M+1]. μ_{eff} (BM) = 1.86; Δ_m (mho cm^2 mol^{-1}) = 18.

3. Results and Discussion

All copper complexes are stable at room temperature, insoluble in water but soluble in DMSO and Methylcyanide. On the isolated solid complexes of Cu(II) ion with the ligands, elemental analysis (C, H, and N), IR, magnetic moments, molar conductance, ^{1}H NMR, and ESR were performed on the isolated solid complexes of Cu(II) ion with the ligands the molecular structures of copper complexes. Analytical ligands'data and their complexes were used to develop the empirical formula for the ligands and their complexes. The elemental analysis of all complexes was good (as shown in the Experimental section). All compounds decomposed above 250 °C, indicating their thermal stability [17].

3.1. *IR spectra*

The IR spectra of the ligands show a ν(C=N) peak in the 1645–1612 cm^{-1} range. All complexes have ν(C= N) bands at 1639–1580 cm^{-1} in their IR spectra [18], which are relocated to lower energy areas in the complexes compared to the free ligands. The change in this band's energy side is most likely due to an increase in the C=N bond order caused by the coordination of nitrogen with the copper atom. Complex spectra exhibit two distinct bands attributable to ν_{asy}(COO-) and ν_{sy}(COO-) at 1630–1600 and 1404–1340 $cm^{-1,}$ indicating that the complexes include the carboxylate oxygen atom. The degree of separation between the $\nu_{asy}(COO^-)$ and $\nu_{sy}(COO^-)$ has also been utilized to determine the carboxylate group coordination mode. In copper complexes, the separation value between ν_{asy} (COO^-) and $\nu_{sy}(COO^-)$ was larger than 200 cm^{-1} (260–216 cm^{-1}), indicating that the carboxylate group in copper complexes of the ligands is coordinated monodentately [19]. In the spectra of copper complexes, the Schiff base ligands show a band about 283 cm^{-1}, attributed to (Cu-Se), which shifts to lower frequencies in the region 253–213 cm^{-1} [20], indicating copper ion coordinated to the selenium atom of the hetero-organoselanyl moiety. Figs. 1 and 2 show the FT-IR spectra of the ligand 2f and its copper chelate 3f. Table 1 shows the characteristic peaks of synthesized ligands and their complexes.

Table 1. IR characteristic peak of synthesized ligands and complexes.

Ligand / complex	ν C=N (cm^{-1})	ν M-N (cm^{-1})	ν $(coo^-)_{ass}$ (cm^{-1})	ν $(coo^-)_{sy}$ (cm^{-1})
2a	1645	-	-	-
2b	1640		-	-
2c	1632	-	-	-
2d	1639	-	-	-
2e	1620	-	-	-
2f	1645	-	-	-
2g	1635	-	-	-
2h	1622	-	-	-
2i	1612	-	-	-
3a	1635	530 – 540	1620	1390
3b	1630	530 – 540	1610	1380
3c	1620	530 – 540	1620	1400
3d	1630	530 – 540	1610	1380
3e	1630	530 – 540	1620	1390
3f	1635	530 – 540	1610	1360
3g	1625	530 – 540	1620	1390
3h	1610	530 – 540	1600	1380
3i	1600	530 – 540	1610	1400

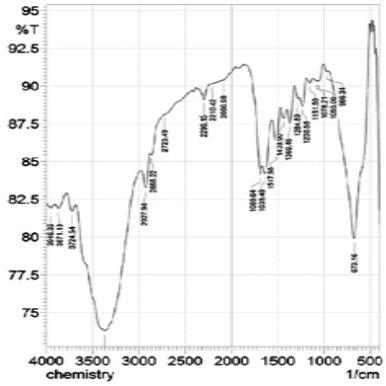

Fig. 1. FTIR spectrum of ligand 2f.

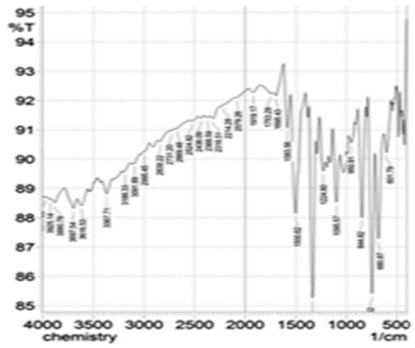

Fig. 2. FTIR spectrum of copper complex 3f.

3.2. *Mass spectra*

Mass spectra are critical for determining compound structure. The mass spectra of the ligands (2c, 2f, 2i) and their copper complexes3c, 3f, 3i (Fig. 3) were recorded, and their stoichiometric compositions were compared. The intensity of these peaks reflects the stability and abundance of the ion [21]. The ligands 2c, 2f, and 2i have a molecular ion peak at 499m/z, 528 m/z, and 536 m/z, while its copper complex has a molecular ion peak at 680 m/z, 709 m/z, and 719 m/z confirming the copper complex stoichiometry of 1:1. Elemental analysis values closely match those estimated from molecular formulae assigned to these complexes, as evidenced by FAB-mass examinations of individual complexes. Similar mass spectrum features were given to other ligands and their copper complexes.

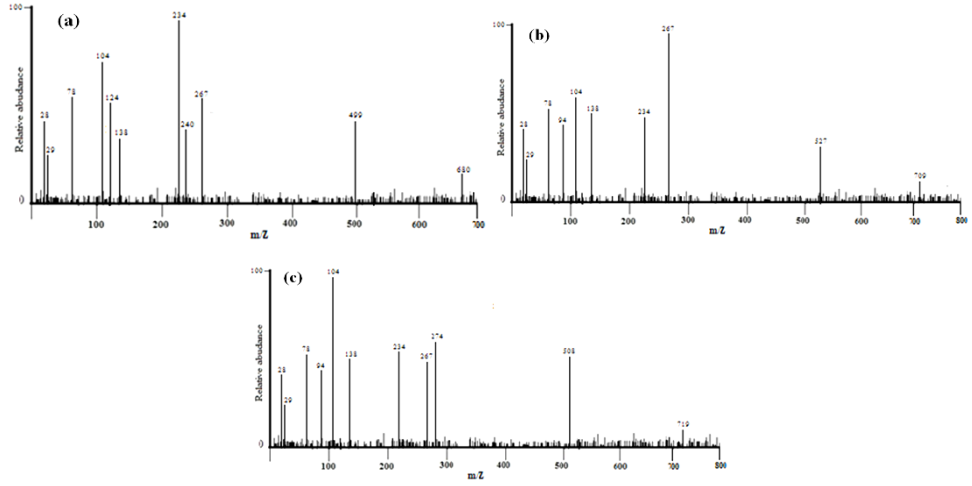

Fig. 3. Mass spectrum of copper complexes a) 3c, b) 3f, and c) 3i.

3.3. *^{1}H NMR Spectra*

The ^{1}H and ^{13}C-NMR spectra of ligands were recorded in $CDCl_3$ and are given in the experimental section. Complex 2f shows (Fig. 4) singlet at δ: 2.28 (s, 6H), 8.34 (s, NH), 6.16 (s, 1H), 6.48 (s, 1H), 6.82 (d, 1H), 6.88 (d, 1H) 6.66-6.72 (m, 5H), 7.25-7.27 (d, 2H), 7.58-7.61 (m, 3H). All the protons were found to be in their expected region [22]. The conclusions drawn from these studies lend further support to the mode of bonding discussed in their IR spectra. The number of protons calculated from the integration curves and those obtained from the values of the expected CHN analyses agrees with each other.

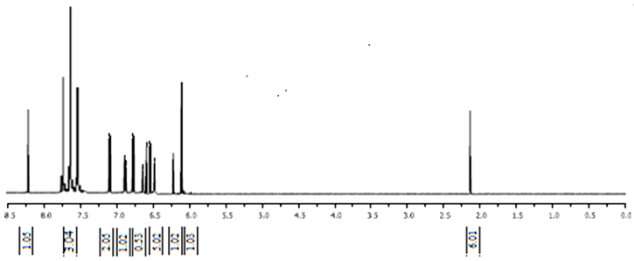

Fig. 4. ^{1}H NMR spectra of ligand 2f.

3.4. *Electronic spectra*

The electronic spectra of the ligands and their complexes were recorded in DMSO as a solvent. The ligand 2f has 224 and 312 nm bands in its absorption spectra. These bands are caused by the n–π * and π–π * transitions within the Schiff base molecule. In DMSO, the electronic spectra of the corresponding complex reveal a band at 556 nm that is indicative of the square planar environment around the copper(II) ion and can be assigned to the $^2B_{1g} \rightarrow {}^2A_{1g}$ transition [23,24]. Similar spectral properties were given to other complexes. The electronic spectra of all the complexes show bands in 200–225, 272–332 and 362–390 nm ranges, which could be due to the benzenoid's π–π* transition or n–π* (COO), the > C=N- chromophore's π–π* transition, and the > C=N- chromophore's n–π* transition, combined with the secondary band of the benzene. Furthermore, there were a few sharp lines in the spectra of the complexes in area 233–257 nm that may be attributable to charge transfer bands. Magnetic susceptibility tests in the solid-state revealed that the copper complexes were paramagnetic at room temperature. These complexes have magnetic moments similar to those expected for copper(II) complexes with no metal-metal interaction. The magnetic moment of the complex 3f at ambient temperature is 1.76 BM, which is typical for mononuclear complexes of magnetically diluted d^9 systems with S = 1/2 spin state and square planar structure, and there is no metal-metal contact along with the axial position. Magnetic behavior was similar in other copper complexes. Figs. 5 and 6 show the UV spectra of ligands 2c, 2f, 2i, and their complexes 3c, 3f, 3i.

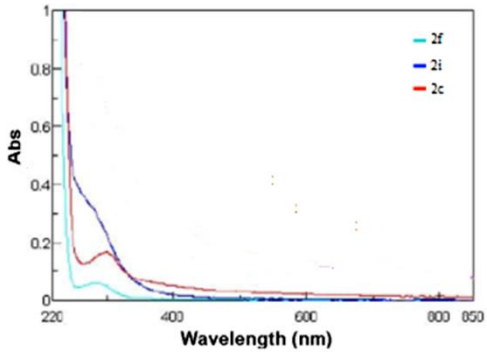

Fig. 5. UV spectra of ligands 2c, 2f and 2i.

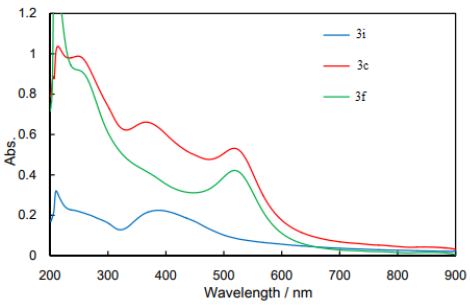

Fig. 6. UV spectra of copper complexes 3c, 3f and 3i.

3.5. *ESR spectra*

The ESR spectra of 3f (Fig. 7) were recorded at 77 K in DMSO solution. The observed g|| value of 2.262 for copper chelate indicates that the metal-ligand link had a covalent character [25]. The planar distortion of Cu(II) chelate due to regular geometrical configurations (f = g||/A||) was computed and found to be 146.2. The results showed that the distortion from regular square planar geometry around the copper center enabled the biomolecular mechanism for biological reactions [26].

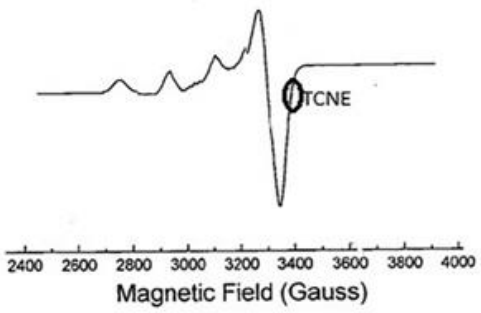

Fig. 7. ESR spectrum of copper complex 3f.

3.6. *Molar conductance*

The copper complexes'molar conductance data measured in 0.001 M DMSO solution was found in the experimental section. The complexes had values between 10 and 29 mho cm^2 mol^{-1}, which is within the predicted range of 1 to 35 mho cm^2 mol^{-1} for non-electrolytes [27]. The complexes are non-electrolytic due to the involvement of the acetate groups in coordination. This was confirmed by a chemical study of the CH_3COO^- ion that was not precipitated by the addition of $FeCl_3$.

3.7. *TGA and DTA studies*

TGA provides key structural data for metal chelate heat stability. The thermogravimetric profile revealed several structural moieties, such as lattice water or coordinated water molecules, anions, molecular fragments after ligand disintegration, and metal oxide as residual chelates. Under nitrogen atmosphere, the thermogravimetric profile of metal complexes was measured up to 750 °C at a heating rate of 10 °C/min. There was no breakdown below 200 °C in the copper complex, indicating no water molecules present. Then, in the temperature range of 260–400 °C, the breakdown was identified, corresponding to the ligand system's partial decomposition. Furthermore, the divergence observed between 340 and 468 °C indicates that complete ligand breakdown results in copper oxide (CuO) as a residue, along with a small amount of ash (Fig. 8).

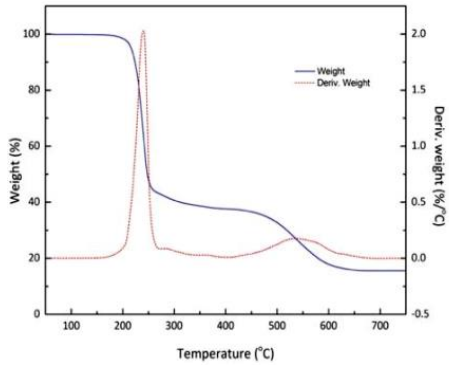

Fig. 8. TGA and DTA curves of copper(II) complex.

3.8. *Antimicrobial activities*

Because of rising antimicrobial resistance, the World Health Organization (WHO) monitors diseases caused by microorganisms such as bacteria and fungi. Metal-based medicines are a viable way to develop novel therapeutics with various modes of action [28]. The goal of disrupting hydrophobic interactions in bacterial plasma membranes, composed of a phospholipid bilayer identical to that seen in eukaryotic cells, brings us back to amphiphilic metal complexes. The synthesized ligands and metal complexes were accessed in the present investigations against the following human pathogen strains: three Gram-negative bacteria, *Proteous vulgaris*, *Klebsiella pneumonia* and *Shigella flexneri*, three Gram-positive bacteria, *Staphylococcus aureus*, *Staphylococcus epidermidis* and *Bacillis subtilis*, and three Fungi, *Aspergillus fumigatus*, *Aspergillus clavatus* and *Candida albicans* shown in Tables 2 and 3. The serial dilution method was used to determine the preliminary antibacterial and antifungal activity screening.

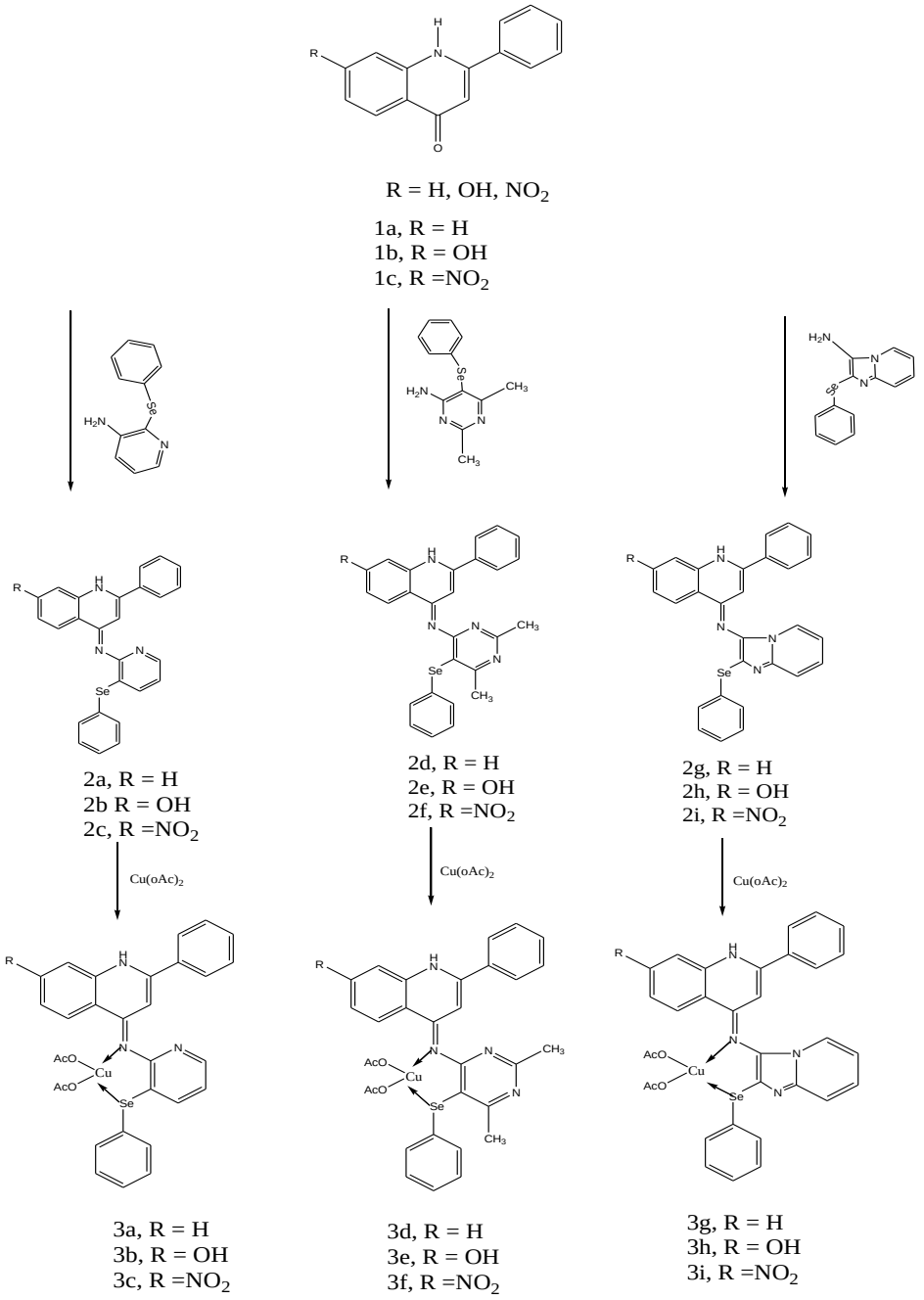

Scheme 1. Synthesis of copper complexes (3a – i).

Antimicrobial tests were carried out by dissolving 5 mg of the chemical compound in 1 mL of dimethyl sulfoxide (DMSO). Gentamycin, Ampicillin, and Amphotericin B (1

mg/mL) were used as standard benchmarks for Gram-negative bacteria, Gram-positive bacteria, and antifungal activity, respectively. Due to chelation [29] and overtone concept [30] via various biochemical actions, inhibitions of protein, RNA, and DNA, the copper chelate 3f is more inhibitory of microbial growth than other chelates and ligand under similar conditions. Because of the differences in the makeup of the cell membranes, the experimental data revealed that the produced metal chelates were more effective against Gram +ve strains than Gram -ve strains. The biological activity of a specific molecule is influenced by a variety of factors, such as lipophilia, resonance, chemical structure, and thermodynamic stability [31,32].

Table 2. Antimicrobial activity of the synthesized complexes against bacteria expressed as inhibition diameter zones in mm based on well diffusion assay.

Complex	Gram +ve bacteria			Gram -ve bacteria		
	B. subtilis	*S. epidermidis*	*S. aureus*	*S. flexneri*	*K. pneumonia*	*P. vulgaris*
3a	8.43	8.09	7.93	7.52	8.63	8.13
3b	11.61	10.52	10.72	9.55	10.42	10.11
3c	14.64	13.62	12.44	12.12	13.52	12.08
3d	10.16	9.14	9.12	9.11	9.98	9.82
3e	13.64	12.62	12.34	11.12	12.52	11.08
3f	16.18	15.12	14.18	14 .43	15.35	13.24
3g	9.54	8.82	8.61	8.24	9.12	8.96
3h	12.88	11.86	11.56	10.73	11.84	11.72
3i	15.98	14.82	13.92	13.85	14.52	12.94
Ampicilin	18.94	16.42	15.65			
Gentamycin				15.43	16.35	14.84

Table 3. Antimicrobial activity of the synthesized complexes against fungi expressed as inhibition diameter zones in millimeters (mm) based on well diffusion assay.

Complex	Fungi		
	C. albicans	*A. fumigatus*	*A. clavatus*
3a	7.96	8.84	8.65
3b	11.06	11.12	10.68
3c	14.96	13.58	13.68
3d	9.68	10.12	9.65
3e	13.96	12.58	12.68
3f	13.18	15.32	15.12
3g	8.69	9.46	9.34
3h	12.68	11.82	11.52
3i	12.86	14.91	14.85
Amphotericin	14.78	16.92	15.42

3.9. *Radical scavenging activity of the synthesized compounds*

The radical scavenging ability of the synthesized complexes was tested using the 1, 1-diphenyl-2-picryl hydrazyl (DPPH). A 0.04 mg/mL DPPH solution in methanol was generated in this technique. 1 mL of this solution was put into 4 mL of synthesized

samples in methanol to achieve four different concentrations (12.5, 25, 50, and 100 g/ mL). Control was made by pouring 1 mL of this solution into 4 mL of methanol, with 4 mL methanol serving as a blank. The mixtures were agitated before being baked for 30 minutes at 37 °C in a dark oven, with absorbance measured with a double beam UV-Vis spectrophotometer at 517 nm. Ascorbic acid was utilized as a standard at the same concentration as above. The % inhibition of the DPPH radical was calculated using the equation below.

$$\% \text{ inhibition} = A_o - A_1 / A_o \times 100$$

A_1 is the absorbance in the presence of a test or standard sample, and A_o is the absorbance of the control reaction [33]. The DPPH assay was extensively used to analyze the ability of synthetic complexes or phytochemicals to scavenge free radicals and determine their antioxidant activity. Antioxidant complexes reduced the absorbance at 517 nm, which is caused by the DPPH radical and their ability to turn DPPH from purple to yellow. The radical scavenging behavior of the synthesized complexes was evaluated using DPPH in this investigation, and the findings are presented in Fig. 9. The coordination of metal in the four positions of the condensed ring system and selenium in the 2f, which increases its capacity to stabilize unpaired electrons and thus scavenge free radicals, could explain complex 3f's high antioxidant activity in comparison to free ligands. Furthermore, the presence of a hetero-organoselenium moiety in the copper complex suggested that complex 3f could be a new interesting lead candidate for future antioxidant design and synthesis.

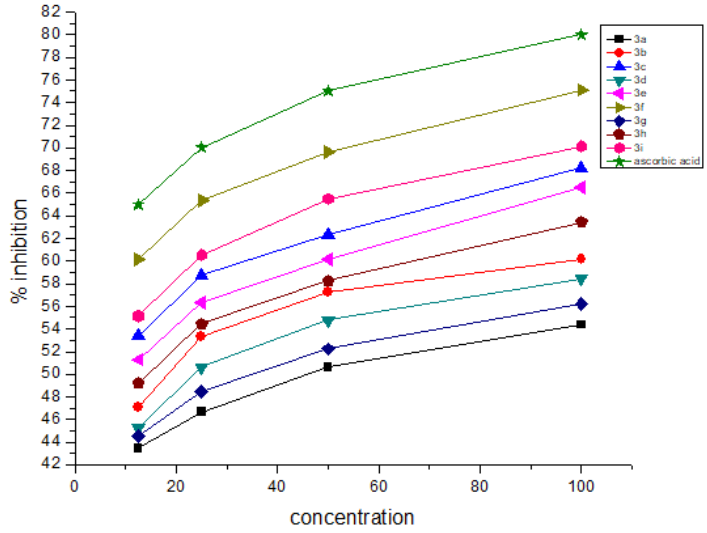

Fig. 9. Percentage inhibition of DPPH radical by the synthetic compounds.

3.10. *Cytotoxicity*

The cytotoxicity of metal chelates (Fig. 10) and ligands on HL-60 and MCF-7 cells was determined after 24 h of incubation. It is dependent on their ability to bind to DNA and damage its structure, resulting in degradation of their function, obstructing replication and transcription, and eventually cell death. The synthesized complexes were tested in vitro for activity against HL-60 and MCF-7 using the MTT assay. The percentage of intact cells was calculated and compared to the control. These compounds' activities against the two cell lines were compared to those of doxorubicin. All compounds suppressed both cells in a dose-dependent manner. Ip *et al*. [34] published comparative tests between comparable sulfur and selenium compounds, demonstrating that selenium inhibits cancer cell development far more effectively than sulfur. Furthermore, selenium may impede cellular transformation through a multi-modal approach. In vitro activity of 3c, 3e, and 3i was moderate in selectivity and as an orientative measure. At 100 mM, 3f was much more active against two cell lines, HL-60 and MCF-7.

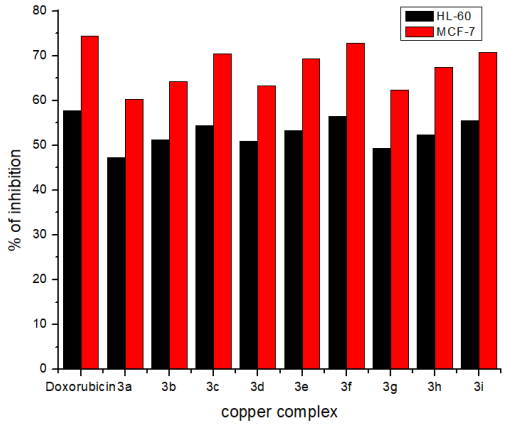

Fig. 10. Cytotoxic activities of the complex against two cancer cell lines.

3.11. *DNA interaction studies*

3.11.1. *Electrochemical studies*

Copper(II) complexes with 2,6-dimethyl-5-(phenylselanyl)pyrimidin-4-amine derivative showed one-electron redox characteristics (Fig. 11), with a Cu^{2+}/Cu^{+} pair at Epa = 0.05 and Epc = 0.20 V. The addition of CT-DNA to the metal chelate resulted in a considerable decrease in both anodic and cathodic current as well as a shift in electrode potential. The gradual change in potential and current revealed that partial intercalation (fused aromatic rings) and partial electrostatic interactions (between the -ve charged phosphate backbone and + ve charged copper ion) were irresponsible for the binding of copper chelate to the

electrode surface. The metal complex had a lot of cytotoxicity against the HL-60 and MCF-7 cell lines, which helped to clarify the DNA binding investigations.

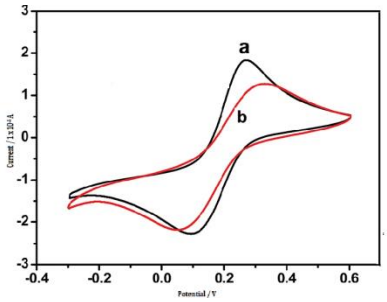

Fig. 11. Cyclic voltammetric behavior of copper complex 3f in the a) absence and b) presence of DNA.

3.11.2. *Viscosity measurements*

The viscosity experiment is useful for determining how well metal complexes bind to DNA. Complexes have a binding affinity for DNA, according to the proportionate changes in viscosity. The DNA helix must be lengthened, and the DNA viscosity must be increased in a classic intercalation mode. By intercalating the double helix of DNA, ethidium bromide, a well-known DNA intercalator, greatly increases relative viscosity. There is a considerable increase in viscosity when DNA is added to metal complexes (Fig. 12). The rise in viscosity indicates that the complexes engage by intercalation binding, supported by electronic spectrum features. The experiment results show that the complex 3f has a higher affinity for binding DNA than other complexes.

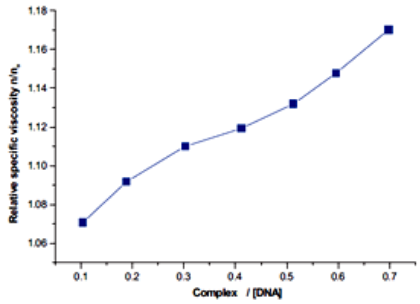

Fig. 12. Effects of the increasing amount of complex 3f on the relative viscosity of CT-DNA at 25 ± 0.1° C.

Conclusion

The synthesis, characterization, and biological evaluation of copper(II) complexes with hetero-organoselenium-based Schiff base ligands 2-(phenylselanyl)pyridine-3-amine, 2,6-

dimethyl-5-(phenylselanyl)pyrimidin-4-amine, and 2-(phenylselanyl)H-imidazo[1,2-α] pyridine-3-amine were investigated in this study. Spectroscopic examinations revealed that the complex connected with two carboxylate oxygen atoms and a copper atom via the quinoline moiety and hetero-organoselenium from the ligand. According to the analytical and spectral data, all copper complexes have a distorted square planar geometry with metal to ligand ratio of 1:1. Electrochemical tests and viscosity measurements were used to evaluate the copper complexes' binding relationship with calf thymus DNA (CT-DNA). All of the complexes reacted with CT-DNA via an intercalation manner. In the antimicrobial study, lipophilic and polar substituents like C=N and Se–N are likely to increase fungal and bacterial toxicity; hence copper(II) complexes have a higher probability of interacting with nucleotide bases. The nitro substituted copper complexes showed good antibacterial, antifungal and anticancer activities due totheir strong electron-withdrawing nature increases the lipophilic character. Furthermore, it was discovered that complexing the ligand with the metal ion improves its anticancer activity in the MCF-7 cell line. Furthermore, incorporating a hetero-organoselenium moiety in the copper complex showed that it could be a new promising lead candidate for future antioxidant design and synthesis.

Acknowledgment

We thank the Head, Department of Chemistry, and Manonmaniam Sundaranar University for providing the necessary facilities.

References

1. S. Mayadevi, P. G. Prasad, and K. K. M. Yusuff, Synth. React. Inorg. Met. Org. Chem. **33**, 481 (2003). http://dx.doi.org/10.1081/SIM-120020000
2. R. N. Prasad, K. M. Sharma, and A. Agrawal, Indian J. Chem. A **46**, 600 (2007). https://doi.org/10.1155/2015/525239
3. R. Johari, G. Kumar, and S. Singh, J. Indian Chem. Soc. **26**, 23 (2009). https://doi.org/10.1016/j.ejmech.2010.03.036
4. A. S. Shekhawat, N. P. Singh, and N. S. Chundawat, J. Sci. Res. **14**, 38 (2022) http://dx.doi.org/10.3329/jsr.v12i1.427457
5. M. G. Kayirere, A. Mahamoud, J. Chevalier, J.C. Soyfer, A. Cŕemieux, and J. Barbe, Eur. J. Med. Chem. **33**, 55 (1998). https://doi.org/10.1016/S0223-5234(99)80076-2
6. R. Musiol, J. Jampilek, and V. Buchta, Bioorg. Med. Chem. **14**, 3592 (2006). https://doi.org/10.1016/j.bmc.2006.01.016
7. M. Jain, S. I. Khan, and B. L. Tekwari, Bioorg. Med. Chem. **13**, 4458 (2005). https://doi.org/10.1016/j.bmc.2005.04.034
8. W. Cunico, C. A. Cechinel, and H. G. Bonacorso, Bioorg. Med. Chem. Lett. **16**, 649 (2006). https://doi.org/10.1016/j.bmcl.2005.10.033
9. Y. L. Chen, C. J. Huang, and Z. Y. Huang, Bioorg. Med. Chem. **14**, 3098 (2006). https://doi.org/10.1016/j.bmc.2005.12.017
10. N. Muruganantham, R. Sivakumar, N. Anbalagan, V. Gunasekaran, and J. T. Leonard, Biol. Pharm. Bull. **27**, 1683 (2004). https://doi.org/10.1248/bpb.27.1683
11. S. W. May and S. H. Pollock, Drugs **56**, 959 (1998). https://doi.org/10.2165/00003495-199856060-00001

12. G. Mugesh, W. W. du Mont, and H. Sies, Chem. Rev. **101**, 2125 (2001). https://doi.org/10.1021/cr000426w
13. M. I. Jackson and G. F. Combs, Curr. Opin. Clin. Nutr. Metab. Care **11**, 718 (2008). http://doi.org/10.1097/MCO.0b013e3283139674
14. H. Xianran, Z. Min, L. Shaolei, L. Xiaolong, L.Yiyan, L. Zhongtang, G. Yangguang, D. Fei, W. Dan, L. Yuchen, and Z. Yongmin, Eur. J. Med. Chem. **208**, ID 112864 (2020). http://doi.org/10.1016/j.ejmech.2020.112864
15. M. N. Schrauzer, Mol. Life Sci. **57**, 1864 (2007). https://doi.org/10.1007/BF02698014
16. A. G. Vogta, G. T. Vossa, and L. Renata, Chem. Biol. Interact. **282**, 7 (2018). https://doi.org/10.1016/j.cbi.2018.01.003
17. C. Adhikary, R. Bera, B. Dutta, S. Jana, G. Bocelli, A. Cantoni, S. Chaudhuri, and S. Koner, Polyhedron **27**, 1556 (2008). https://doi.org/10.1016/j.poly.2008.01.030
18. A. D. Bansod, R. G. Mahale, and A. S. Aswar, Russ. J. Inorg. Chem. **52**, 879 (2007). https://doi.org/10.1134/S0036023607060113
19. K. Nakamoto, Spectroscopy and Structure of Metal Chelate Compounds (John Wiley, New York, 1988).
20. I. M. Charemisina, E. V. Khiystunova, and V. L. Varand, Acad. Sci. USSR **12**, 2672 (1972). https://doi.org/10.1007/BF00849822
21. M. Hamming, N. Foster, Interpretation of Mass Spectra of Organic Compounds (Academic Press: New York, 1972).
22. Y. J. Liu, N. Wang, W. J. Mei, F. Chen, F, L. X. He, L. Q. Jian, and F. H .Wu, Transit. Met. Chem. **32**, 332 (2007). https://doi.org/10.1007/s11243-006-0172-4
23. S. Chandra and L. K. Gupta, Spectrochim. Acta A Mol. Biomol. **61**, 269-275, (2005). https://doi.org/10.1016/j.saa.2004.03.040
24. A. B. P. Lever, Inorganic Electronic Spectroscopy, 2nd Edition (Elsevier, New York, 1968).
25. A. S. Gaballa, M. S. Asker, A. S. Barakat, and S. M. Teleb, Spectrochim. Acta A Mol. Biomol. **67**, 114 (2007). https://doi.org/10.1016/j.saa.2006.06.031
26. M. Fujiwara, H.Watika, T. Matsushtla, and T. Shono, Bull. Chem. Soc. Jpn. **63**, ID 3443 (1990). https://doi.org/10.1246/bcsj.63.3443
27. W. J. Geary, Coord. Chem. Rev. **7**, 81 (1971). https://doi.org/10.1016/S0010-8545(00)80009-0
28. M. G. Rabbani and M. R. Islam, J. Sci. Res. **13**, 545 (2021). http://dx.doi.org/10.3329/jsr.v13i2.49508
29. S. Ramakrishnan, V. Rajendiran, M. Palaniandavar, V. S. Periasamy, B. S. Srinag, H. Krishnamurthy, and M. A. Akbarsha, Inorg. Chem. **484**, 1309 (2009). https://doi.org/10.1016/j.ica.2018.09.044
30. M. Ganeshpandian, R. Loganathan, S. Ramakrishnan, A. Riyasdeen, M. A. Akbarsha, and M. Palaniandavar, Polyhedron **52**, 924 (2013). https://doi.org/10.1016/j.poly.2012.07.021
31. F. Arjmand, S. Parveen, M. Afzal, and M. Shahid, J. Photochem. Photobiol. B Biol. **114**, 15 (2012). https://doi.org/10.1016/j.jphotobiol.2012.05.012
32. Z. A. Siddiqi, P. K. Sharma, M. Shahid, S. Kumar, and A. Siddique, Spectrochim. Acta A Mol. Biomol. **93**, 280 (2012). https://doi.org/10.1016/j.saa.2012.03.009
33. R. Subashini, S. M. roopan, and F. N. khan, J. Chil. Chem. Soc. **55**, 317 (2010). http://dx.doi.org/10.4067/S0717-97072010000300008
34. C. Ip and H. E. Ganther, Carcinogenesis **13**, 1167 (1992). https://doi.org/10.1093/carcin/13.7.1167